
From Learning to Optimize to Learning Optimization Algorithms

Camille Castera*

University of Tübingen
Tübingen, Germany

camille.castera@protonmail.com

Peter Ochs

Saarland University
Saarbrücken, Germany

ochs@cs.uni-saarland.de

Abstract

Towards designing learned optimization algorithms that are usable beyond their training setting, we identify key principles that classical algorithms obey, but have up to now, not been used for Learning to Optimize (L2O). Following these principles, we provide a general design pipeline, taking into account data, architecture and learning strategy, and thereby enabling a synergy between classical optimization and L2O, resulting in a philosophy of *Learning Optimization Algorithms*. As a consequence our learned algorithms perform well far beyond problems from the training distribution. We demonstrate the success of these novel principles by designing a new learning-enhanced BFGS algorithm and provide numerical experiments evidencing its adaptation to many settings at test time.

1 Introduction

Learning to Optimize (**L2O**) is a modern and promising approach towards designing optimization algorithms that reach a new level of efficiency. L2O is even the state-of-the-art approach in some applications [44, 75]. However, it mostly excels when designed and trained specifically for each application and still fails to be widely applicable without retraining models. This need to adapt L2O specifically to each task is especially problematic given how difficult designing L2O algorithm is: the design is prone to many conceptual pitfalls and training models is not only computationally expensive [16] but also notoriously hard in L2O [49]. In contrast, standard optimization methods are widely applicable, sometimes way beyond the setting they were originally designed for, as attested for example by the success of momentum methods [55] in deep learning [34]. This transfer of performance to different classes of problems is often achieved only at the cost of tuning a few scalar hyper-parameters. Analytically designed optimization algorithms usually come with theoretical guarantees, which most L2O algorithms lack completely.

We aim to bring L2O models closer to actual Learned Optimization Algorithms (**LOAs**), that are applicable far beyond their training setting. This is achieved by identifying key theoretical principles that standard optimization algorithms follow and by providing strategies ensuring that LOAs inherit these properties. Thereby we systematically unify the advantages of both worlds: flexible applicability and theoretically controlled convergence guarantees from mathematical optimization, and complex operations from machine learning beyond what can be analytically designed. Following our general recipe, we derive a learning-enhanced BFGS [11, 19, 24, 62] method. We present numerical and theoretical results that show how our LOA benefits from our approach.

*Corresponding author.

2 Setting and Problem Statement

We first develop a mathematical and algorithmic formulation of the L2O setting that we are interested in and then state the problem we study within this formalism.

2.1 Mathematical Formalism

We denote by \mathbb{N} the set of non-negative integers and \mathbb{R} the set of real numbers. In what follows we consider unconstrained optimization problems of the form

$$\min_{x \in \mathbb{R}^n} f(x),$$

where $n \in \mathbb{N}$ is the dimension of the problem, and f belongs to \mathfrak{F}_n , the set of real-valued lower bounded twice-continuously differentiable functions on \mathbb{R}^n (equipped with inner product $\langle \cdot, \cdot \rangle$ and norm $\|\cdot\|$). We denote by ∇f and $\nabla^2 f$ the gradient and Hessian matrix of f respectively.

One of our goals is to design LOAs that are applicable in any dimension (see Principle 1 below), like standard optimization algorithms. Therefore in the sequel, the dimension n is arbitrary and need not be the same for all the problems the algorithms are applied to. Nevertheless, for the sake of simplicity, the following discusses a fixed \mathbb{R}^n . A triplet (f, x_0, S_0) with an objective function $f \in \mathfrak{F}_n$, an initialization $x_0 \in \mathbb{R}^n$ and a collection of vectors and matrices $S_0 \in \mathfrak{S}_n$, called *state* (where \mathfrak{S}_n is the set of all possible states, to be clarified hereafter), is called a *problem*.

We formulate L2O algorithms in a generic form described in Algorithm 1 that takes as input a problem (f, x_0, S_0) and performs $K \in \mathbb{N}$ iterations before returning $x_K \in \mathbb{R}^n$. Algorithm 1 can also be mathematically represented by an operator from $\mathcal{A}: \mathfrak{F}_n \times \mathbb{R}^n \times \mathfrak{S}_n \times \mathbb{N} \rightarrow \mathbb{R}^n$ such that the K -th iteration of the algorithm reads

$$x_K = \mathcal{A}(f, x_0, S_0, K).$$

Algorithm 1 is fully characterized by what we call an *oracle* \mathcal{C} , a *model* \mathcal{M} , an *update* function \mathcal{U} and a *storage* function \mathcal{S} . At any iteration $k \in \mathbb{N}$, the oracle \mathcal{C} collects the information the algorithm has access to about f at the current point x_k and the state S_k and constructs an *input* $I_k \in \mathbb{R}^{n \times n_i}$, where $n_i \in \mathbb{N}$. The input I_k is then fed to a (machine learning) model represented by a parametric function $\mathcal{M}(\cdot, \theta): \mathbb{R}^{n \times n_i} \rightarrow \mathbb{R}^{n \times m}$, where $\theta \in \mathbb{R}^p$ ($p \in \mathbb{N}$) is its parameter (in vector form), and $m \in \mathbb{N}$. The model outputs a *prediction*, i.e., $y_k = \mathcal{M}(I_k, \theta)$, which is used by the update $\mathcal{U}: \mathbb{R}^{n \times n_i} \times \mathbb{R}^{n \times m} \times \mathbb{R}^{n_h}$ to improve the current point: $x_{k+1} = x_k + \mathcal{U}(I_k, y_k, \Gamma)$, where $\Gamma \in \mathbb{R}^{n_h}$ ($n_h \in \mathbb{N}$) are the hyper-parameters chosen by the user (a few scalars). The storage \mathcal{S} then collects in S_{k+1} the information from the k -th iterate that will be used at the next iteration. This abstract formalism is generic enough to encompass at the same time L2O and several classical algorithms. Moreover, this systematic structuring allows for the formulation and analysis of key principles for learned optimization algorithms in Section 3. We now illustrate this on an example.

Algorithm 1: Generic Learned Optimization Algorithm

given: oracle operator \mathcal{C} , model $\mathcal{M}(\cdot, \theta)$, update function \mathcal{U} , storage function \mathcal{S}

input: function to minimize f , initialization x_0 , state S_0 , hyper-parameter Γ , number of iterations K

for $k = 0$ to $K - 1$:

$I_k \leftarrow \mathcal{C}(f, x_k, S_k)$	// Construct input
$y_k \leftarrow \mathcal{M}(I_k, \theta)$	// Model prediction
$x_{k+1} \leftarrow x_k + \mathcal{U}(I_k, y_k, \Gamma)$	// Update step
$S_{k+1} \leftarrow \mathcal{S}(S, x_k, I_k, y_k)$	// Store relevant variables in state

return x_K

Example: Throughout what follows we use the heavy-ball (HB) method [55] as running example to illustrate the concepts we introduce. An iteration $k \in \mathbb{N}$ of HB reads:

$$x_{k+1} = x_k + \alpha d_k - \gamma \nabla f(x_k), \quad (1)$$

where $d_k = x_k - x_{k-1}$, $\alpha \in [0, 1)$ is called the momentum parameter and $\gamma > 0$ is the step-size. Notice that for $k = 0$, the algorithm requires not only x_0 but also x_{-1} . This is the reason for

introducing a state in Algorithm 1, in this case we would have $S_0 = \{x_{-1}\}$. Any iteration k of HB reads as follows: the operator \mathcal{C} takes (f, x_k, S_k) , where $S_k = \{x_{k-1}\}$, and concatenates $\nabla f(x_k)$ and d_k as $I_k = (d_k, \nabla f(x_k)) \in \mathbb{R}^{n \times n_i}$, with $n_i = 2$. There is no learning phase hence no model \mathcal{M} (by convention we say that $m = 0$ and $y_k = 0$). The update function \mathcal{U} has hyper-parameter $\Gamma = (\alpha, \gamma)$ —so $n_h = 2$ —and uses I_k to compute $\mathcal{U}(I_k, 0, \Gamma) = \alpha d_k - \gamma \nabla f(x_k)$, which yields the update (1). Finally, the storage \mathcal{S} stores x_k in S_{k+1} , as it will be required to compute d_{k+1} .

2.2 The Stages of L2O vs LOA

Training phase: The parameter θ of the model \mathcal{M} is set by building a *training set* of problems (f, x_0, S_0) and by minimizing a *loss function* on this dataset, e.g., the value $f(x_K)$ achieved on average after K iterations. Training is crucial to find a “good” θ but is computationally expensive and notoriously hard in L2O [69, 49]. Therefore our work studies the case of training the model on a fixed training set, after which the algorithm can be directly applied to any $f \in \mathfrak{F}_n$ without retraining.

Test phase: In machine learning, the standard assumption is that the training set is sampled from an unknown underlying distribution of problems. Generalization, in the statistical sense, then refers to asserting how good the trained model $\mathcal{M}(\cdot, \theta)$ performs on the whole distribution. This is estimated by computing the performance on a *test set* sampled independently from the same distribution.

Generalization: As motivated in introduction, we aim for learned algorithms that perform well on settings possibly significantly different from that of the training set. This is sometimes referred to as out of distribution (OOD) generalization. We do not pursue OOD generalization, which is hopeless in full generality [71]. In fact, *this is where we draw the line between L2O and LOA*: instead of studying generalization from a statistical perspective, we list use cases to which one wants L2O algorithms to be adaptable to, since successful standard algorithms are. Firstly, we want algorithms that are applicable to some functions f and initializations not belonging to the training set only by tuning the hyper-parameter Γ . This is more reasonable than OOD generalization. For example, HB was originally designed for locally C^2 functions [55], but works on larger classes of convex functions [23] and even performs well on non-convex ones [73]. It also does not require a specific initialization strategy and convergence rates are uniform in the dimension n [56, 9]. Finally, although for a given f some choices of hyper-parameters (α, γ) might be optimal for HB (see e.g., [52]), the range of admissible values for which it converges is usually larger.

3 Principles of Learning Optimization Algorithms and Consequences

The cornerstone principle of LOA, is that optimization algorithms should be applicable in any dimension n . Since we do not retrain the model $\mathcal{M}(\cdot, \theta)$, this implies the following.

Principle 1. *Algorithm 1 should be independent of the dimension n , i.e., the size p of θ and n_i should be independent of n and as small as possible.*

This principle creates the *main shift between L2O and LOA*: while L2O models might be used for specific applications, making it possible to choose p larger than n , LOAs must work at any scale, putting LOAs in the *under-parameterized* learning setting (p smaller than n). This implies that the training phase cannot be used to memorize a large number of examples like in over-parameterized settings [74], which makes generalizing (Section 2.2) significantly more challenging. We propose to cope with this via a careful algorithmic design articulated around three ideas.

Enhancement: We use learning to enhance existing algorithms, preserving their theoretically-grounded parts and using learning to replace the parts of that are based on heuristics, eventually reducing the size of θ .

Adaption: LOAs must adapt *on the fly* (along the iterates) to each problem by storing information in the state S_k . This can be achieved by recurrent neural networks, e.g., LSTMs [3, 30] or by enhancing adaptive algorithms like ADAM [37] or quasi-Newton (QN) methods, as we do in Section 4.

Hard-coded generalization: We identify key transformations of optimization problems to which standard optimization algorithms are robust to and “hard-code” this robustness (*i.e.*, enforce it by design) in LOAs. Enforcing such robustness avoids wasting parts of θ relearning it and is one of the main contributions of our work. We now explain how to achieve this.

Table 1: Summary of invariance and equivariant properties of several algorithms³

	Translation (Principle 2)	Permutation (Principle 3)	Orthogonal transform.	Geom. scaling (Principle 4)	Func. scaling (Principle 5)
Gradient desc.	✓	✓	✓	dep. Γ	dep. Γ
Heavy-Ball	✓	✓	✓	dep. Γ	dep. Γ
Newton Meth.	✓	✓	✓	✓	✓
BFGS	✓	✓	✓	✓ ²	✓ ²
ADAM [37]	✓	✓	✗	✗	~
Algorithm 2	✓	✓	✗	✓ ²	✓ ²

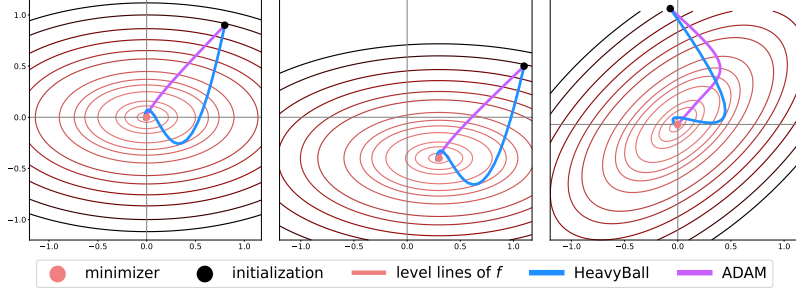


Figure 1: Illustration of equivariances on the landscape of a two-dimensional function. Left: no transformation, middle: translation, right: rotation. Transforming f and x_0 does the same to the iterates of HB. ADAM [37] is also translation equivariant but not rotation equivariant.

3.1 Hard-coding of Generalization

Fix $f \in \mathfrak{F}_n$, $x_0 \in \mathbb{R}^n$ and S_0 and consider an invertible mapping $\mathcal{T}: \mathbb{R}^n \rightarrow \mathbb{R}^n$. Since \mathcal{T} is invertible, observe that for all $x \in \mathbb{R}^n$:

$$f(x) = f(\mathcal{T}^{-1}(\mathcal{T}(x))) = f \circ \mathcal{T}^{-1}(\mathcal{T}(x)) = \hat{f}(\hat{x}), \quad (2)$$

where we define \hat{f} as $f \circ \mathcal{T}^{-1}$ and $\hat{x} = \mathcal{T}(x)$, for all $x \in \mathbb{R}^n$. Therefore (2) expresses in particular that (f, x_0, S_0) and $(\hat{f}, \hat{x}_0, \hat{S}_0)$ are *two different representations of the same problem*, where \hat{S}_0 is one-to-one with S_0 such that for every vector² $\hat{v} \in \hat{S}_0$ there exists $v \in S_0$ such that $\hat{v} = \mathcal{T}(v)$. From a generalization perspective, we want Algorithm 1 to perform the same regardless the representation, *i.e.*,

$$f(\mathcal{A}(f, x_0, S_0, K)) = \hat{f}(\mathcal{A}(\hat{f}, \hat{x}_0, \hat{S}_0, K)), \quad \forall K \in \mathbb{N}.$$

According to (2), this is the case if $\mathcal{A}(\hat{f}, \hat{x}_0, \hat{S}_0, K) = \mathcal{T}(\mathcal{A}(f, x_0, S_0, K))$ for all (f, x_0, S_0) and K . When this is true, we say that the algorithm \mathcal{A} is *equivariant to \mathcal{T}* . While in theory equivariance with respect to all invertible transformations seems best, this imposes severe restrictions to the design of Algorithm 1 and does not actually hold for standard algorithms. Therefore, we analyze equivariance only with respect to key transformations, summarized in Table 1. The complete list is only achieved by Newton’s method, which is unsuitable for large-scale optimization. In the following, we discuss equivariance of Algorithm 1 and how to enforce it by design.

3.1.1 Translations

Let $v \in \mathbb{R}^n$, the translation \mathcal{T}_v is defined for all $x \in \mathbb{R}^n$ by $\mathcal{T}_v(x) = x + v$. In this case $\hat{f} = f(\cdot - v)$ and $\hat{x}_0 = x_0 + v$. Most algorithms are translation equivariant as summarized in Table 1 and illustrated on Figure 1, which leads to the following principle.

Principle 2. *Algorithm 1 should be translation equivariant, i.e., \mathcal{T}_v -equivariant for all $v \in \mathbb{R}^n$.*

²The case of matrices contained in S_0 is more complex and discussed in Appendix B.

³The symbol **dep. Γ** indicates that scale invariance depends on Γ , see Appendix A. ADAM is scale invariant only when its numerical stability parameter is set to 0. The case of BFGS is discussed at the end of Section 4.2.

Strategy. Remark that since $\hat{x}_0 = x_0 + v$, then $\hat{x}_K = x_K + v \iff \sum_{k=0}^{K-1} \hat{d}_k = \sum_{k=0}^{K-1} d_k$. So we want to ensure that $\forall k \in \mathbb{N}$, $d_k = \hat{d}_k$. Looking at the example of HB, it relies on $\nabla f(x_k)$ and $d_k = x_k - x_{k-1}$. One can show (see Appendix A) that $\nabla \hat{f}(\hat{x}) = \nabla f(x)$ and similarly $\hat{x} - \hat{y} = x - y$ for all $x, y \in \mathbb{R}^n$. These quantities are thus *invariant* by translation which makes HB translation equivariant. This example shows that it is often possible to make \mathcal{C} translation invariant (i.e., $\mathcal{C}(f, x, S) = \mathcal{C}(\hat{f}, \hat{x}, \hat{S})$) which is then enough to make the algorithm translation equivariant, since by direct induction $\hat{y}_k = \mathcal{M}(\hat{I}_k, \theta) = \mathcal{M}(I_k, \theta) = y_k$ and thus $\mathcal{U}(\hat{I}_k, \hat{y}_k, \Gamma) = \mathcal{U}(I_k, y_k, \Gamma)$.

Practical consequences. An easy way to ensure translation invariance of \mathcal{C} is to never output “absolute” quantities such as x_k but always differences such as $d_k = x_k - x_{k-1}$, exactly like in the example of HB above. We follow this strategy as it does not put any restriction on \mathcal{M} nor \mathcal{U} .

3.1.2 Permutations

In optimization, the ordering of coordinates is arbitrary in general. For example, the functions $(x, y) \mapsto x^2 + 2y^2$ and $(x, y) \mapsto 2x^2 + y^2$ represent the same problem with permuted coordinates. This transformation is represented by a *permutation matrix* P which contains only zeros except one coordinate equal to 1 per line, and such that $P^T P = \mathbb{I}_n$ where \mathbb{I}_n denotes the identity matrix of size n . Fix such P and consider the corresponding transformation (with \hat{f} and \hat{x} redefined accordingly). As shown in Table 1, almost all popular algorithms are permutation equivariant.⁴

Principle 3. *Algorithm 1 should be equivariant to all permutation matrices P .*

Strategy. Remark that this time to get $\hat{x}_k = P x_k$ for all $k \in \mathbb{N}$, we need $\hat{d}_k = P d_k$ i.e. we need equivariance. Taking again the example of HB, we show in Appendix A that $\nabla \hat{f}(\hat{x}) = (P^{-1})^T \nabla f(x) = P \nabla f(x)$, and we should expect $\hat{d}_k = P d_k$ (since this is what we want to obtain). Therefore we expect \mathcal{C} to be equivariant to permutations this time. This is enough to make HB permutation equivariant. In the context of L2O, since $\mathcal{M}(\hat{I}_k, \theta) = \mathcal{M}(P I_k, \theta)$, we will make $\mathcal{M}(\cdot, \theta)$ equivariant as well so that \mathcal{U} gets only permuted quantities, and design \mathcal{U} to preserve equivariance.

Practical consequences. Permutation equivariance of \mathcal{M} strongly restricts its design as Zaheer et al. [72] showed that the only feed-forward (FF) layer operating along the dimension n and preserving equivariance is very basic with only two learnable parameters and no bias. To be usable in any dimension n , many L2O algorithms use models \mathcal{M} that perform per-coordinate predictions [3], making them permutation equivariant but completely neglecting interactions between coordinates. In Section 4 we rather propose a model that is permutation equivariant while allowing such interactions.

The orthogonal group. Permutations matrices form a subset of the set of orthogonal matrices (square matrices with $P^T P = \mathbb{I}_n$). They correspond to so-called *rotations* and *reflections*. Several algorithms are equivariant to all orthogonal transformations, which makes this property desirable. Yet, it is hardly compatible with L2O since it does not hold for any FF layer with ReLU activation function (as we prove in Appendix A.4). Fortunately, in many setting the canonical coordinate system has a clear meaning (e.g. each coordinate represents a weight of a neural network to train), in which case this equivariance is not crucial, as the performance of ADAM in deep learning attests.

3.1.3 Rescaling

Let $\lambda > 0$ and consider the geometric rescaling $\mathcal{T}_\lambda(x) = \lambda x$, and redefine \hat{f} and \hat{x} accordingly.

Principle 4. *Algorithm 1 should be equivariant to geometric rescaling.*

This principle should be considered as optional as it is usually not satisfied by first-order methods (see Table 1). Indeed, one can see that $\hat{f}(\hat{x}_k) = \frac{1}{\lambda} \nabla f(x)$ and we want $\hat{d}_k = \lambda d_k$. So for example in HB, one needs to tune (α, γ) to recover equivariance. However, Newton’s and QN methods can be equivariant to geometric rescaling. In the context of LOA, we construct an algorithm (in Section 4) where we make \mathcal{M} scale equivariant and show that our update \mathcal{U} can then make Principle 4 hold. This slightly restricts \mathcal{M} , for example the ReLU function is scale equivariant but the sigmoid is not.

⁴A notable exception regards algorithms constructing block-diagonal matrices like K-FAC [46], these blocks depend on the ordering of coordinates.

There is a last, different, principle. For $\lambda > 0$, if this time *the function* is rescaled: $\hat{f} = \lambda f$, then $\nabla \hat{f} = \lambda \nabla f$. This does not transform the optimization variable: $\hat{x}_0 = x_0$ so this time we want *invariance* of the algorithm (and function values are equivariant).

Principle 5. *Algorithm 1 should be such that $\mathcal{A}(\lambda f, x_0, \hat{S}_0, K) = \mathcal{A}(f, x_0, S_0, K)$, $\forall \lambda > 0$.*

For very similar reasons as geometric rescaling, this principle needs to be dealt with specifically for each algorithm. It is also compatible with LOA as we show for our algorithm (see Theorem 1).

4 Application to Learning Quasi-Newton Algorithms

We build a LOA, based on the structure of the BFGS method, that provably obeys the principles identified above. BFGS is a quasi-Newton (QN) method, *i.e.*, one that progressively builds an approximation of the computationally-expensive inverse Hessian matrix used in Newton’s method. This is thus in line with our idea to adapt to each problem *on the fly* (see Section 3). While combining L2O and QN methods has been explored in the literature (see Section 6), our approach differs in several aspects starting with the following.

4.1 A variational view on the BFGS algorithm

Let $k \in \mathbb{N}$ be an iteration, we use the notation $\Delta g_k = \nabla f(x_k) - \nabla f(x_{k-1})$ and recall that $d_k = x_k - x_{k-1}$. QN methods are based on the fact that for quadratic functions $d_k = \nabla^2 f(x_k)^{-1} \Delta g_k$, which is called the *secant equation*. QN methods aim to iteratively build approximations B_k to $\nabla^2 f(x_k)^{-1}$ with the constraint that the secant equation must hold: $d_k = B_k \Delta g_k$ and that B_k is symmetric. From a variational perspective, [25, 24] showed that BFGS aims to keep B_k close to the previous approximation B_{k-1} by taking B_k as the solution of the following problem:

$$B_k = \min_{\substack{B \in \mathbb{R}^{n \times n} \\ s.t. B_k \Delta g_k = d_k \text{ and } B_k - B_{k-1}^T = 0}} \|B - B_{k-1}\|_W. \quad (3)$$

Here $\|\cdot\|_W$ denotes the Frobenius norm reweighted by some symmetric positive definite matrix W . Denoting $y_k = W^{-1} \Delta g_k$ and $r_k = d_k - B_{k-1} \Delta g_k$, one can show that the solution of (3) is

$$B_k = B_{k-1} + \frac{1}{\langle \Delta g_k, y_k \rangle} \left[r_k y_k^T + y_k r_k^T - \frac{\langle \Delta g_k, r_k \rangle}{\langle \Delta g_k, y_k \rangle} y_k y_k^T \right]. \quad (4)$$

BFGS is then based on the heuristic (albeit elegant) trick that taking W^{-1} to be the *unknown* next approximation B_k , yields $y_k = d_k$ (due to the secant equation) and preserves positive-definiteness. Instead of using L2O to directly predict the matrix B_k as done in prior work, we use L2O precisely at this stage to predict a better choice for W^{-1} . However, since W only appears through the vector $y_k = W^{-1} \Delta g_k$, we reduce the computational cost by designing a model \mathcal{M} that *predicts directly* y_k and not W . This allows enhancing BFGS with L2O while preserving the coherence of the algorithm.

4.2 Our Learned Algorithm

We now detail our algorithm, which is also described in Algorithm 2 in the appendix.

The oracle \mathcal{C} . For each iteration $k \in \mathbb{N}$ of our algorithm, we use the state $S_k = \{x_{k-1}, \nabla f(x_{k-1}), B_{k-1}\}$. Our oracle \mathcal{C} computes $\nabla f(x_k)$, d_k and Δg_k as in BFGS but also new features $B_{k-1} \Delta g_k$ and $-\gamma B_{k-1} \nabla f(x_k)$, gathered as $I_k = (B_{k-1} \Delta g_k, d_k, -\gamma B_{k-1} \nabla f(x_k))$. Note that all these features must be scale invariant since B_{k-1} approximates $\nabla^2 f(x_k)^{-1}$.

The learned model \mathcal{M} . Our model only takes three features as input ($n_i = 3$) but creates additional ones by applying a block of coordinate-wise FF layers, then averaging the result and concatenating it to I_k . This allows feature augmentation and makes each coordinate interacting with all the others. The result is then fed to another coordinate-wise block of FF layers added to a linear layer yielding the output $y_k \in \mathbb{R}^n$. The architecture is detailed in Figure 2. The linear layer acts as a skip-connection and will allow us to introduce a trick that stabilizes the training later in Section 5. Note that the cost of each operation inside \mathcal{M} is proportional to n which is cheaper than the matrix-vector products of cost $O(n^2)$ that \mathcal{C} and \mathcal{U} (and vanilla BFGS) involve.

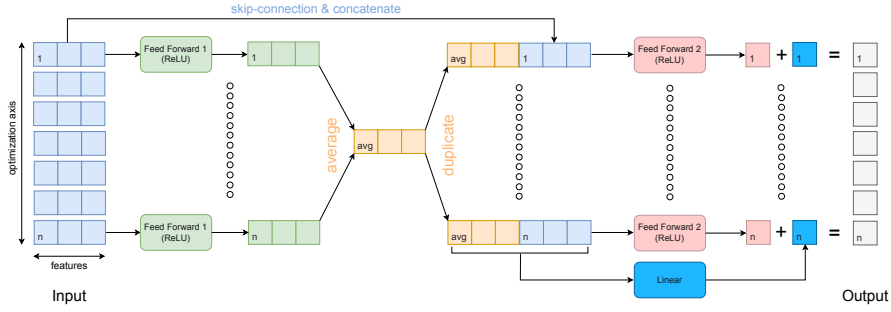


Figure 2: Architecture of our L2O model that preserves the principles of Section 3.1 while computing interactions between coordinates by transforming I_k (in green) and then averaging (in orange).

The update \mathcal{U} and storage \mathcal{S} . Our update is that of BFGS:⁵ the approximation B_k is updated using (4) with a different y_k , and $x_{k+1} = x_k - \gamma B_k \nabla f(x_k)$, where γ is a step-size, usually close to 1 (or chosen by line-search). Like in vanilla BFGS, \mathcal{S} finally stores $\{x_k, \nabla f(x_k), B_k\}$ for the next iterate.

Initialization of B_{-1} . QN methods require an initial approximated inverse Hessian matrix B_{-1} . While the simplest choice is \mathbb{I}_n , several works [7, 8] observed notable improvement by initializing with the Barzilai-Borwein (BB) step-size [6]: $\gamma_{\text{BB}}^{(0)} \stackrel{\text{def}}{=} \frac{\langle \Delta g_0, d_0 \rangle}{\|\Delta g_0\|^2}$. We follow this approach and take $B_{-1} = 0.8\gamma_{\text{BB}}^{(0)}\mathbb{I}_n$. With this choice, B_{-1} agrees with Principles 4 and 5 *without additional knowledge on f* (see Appendix B). This is key to preserve scale invariance of our algorithm (and that of BFGS).

4.3 Theoretical Analysis

Based on our strategy from Section 3, our LOA follows the principles therein, as proved in Appendix B.

Theorem 1. *With the choice of B_{-1} above, Algorithm 2 follows Principles 1-2-3-4-5.*

Another benefit of preserving and enhancing existing algorithms is that their coherent structures allow deriving convergence results, as proved in Appendix C.

Theorem 2. *Assume that f has L -Lipschitz continuous gradient and that for all $k \in \mathbb{N}$, B_k is positive definite with eigenvalues upper-bounded by $C > 0$. Then for any step-size $\gamma \leq \frac{2}{CL}$, $(f(x_k))_{k \in \mathbb{N}}$ converges and $\lim_{k \rightarrow +\infty} \|\nabla f(x_k)\| = 0$.*

It is important to note that Theorem 2 is more restrictive than usual convergence theorems. It is indeed based on strong assumptions regarding the eigenvalues of the matrices $(B_k)_{k \in \mathbb{N}}$. Yet, the result expresses that B_k is the only possible reason for the failure of the algorithm. Additionally, since B_k is constructed based on the output of the model \mathcal{M} , the failure can only come from the learning part of the algorithm. One could thus provide statistical guarantees on the assumption (but only valid for the train/test sets) or enforce the assumption by design of \mathcal{M} [51]. This would put additional restrictions on the model and does not seem necessary in the experiments below.

5 Numerical Experiments and Practical Considerations

In addition to the design choices that we already made to follow our principles (special models, use of ReLU, no bias in FF layers, etc.), we detail some practical considerations that ease the training of our model \mathcal{M} . In what follows assume that we have a dataset of $D \in \mathbb{N}$ problems indexed by superscripts (f^d, x_0^d, S_0^d) , for $d = 1, \dots, D$. For each problem we run the algorithm for $K \in \mathbb{N}$ iterations and denote by $(x_k^d)_{k \in \{0, \dots, K\}}$ the resulting sequence of iterates.

⁵Technically, BFGS and our algorithm would need \mathcal{U} to also take S_k in input to fit in our mathematical formalism. Since this would not affect any of the discussion above, we ignored this for the sake of simplicity.

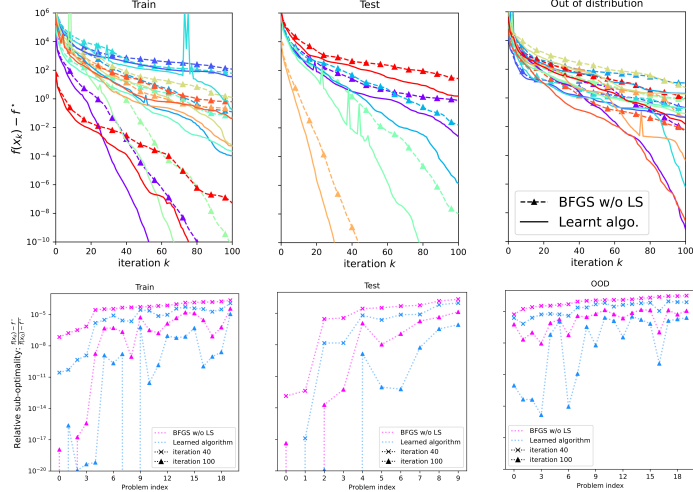


Figure 3: Performance of our learned BFGS method on quadratic functions in dimension $n = 100$. Top row: sub-optimality gap against iterations on the training, test and OOD sets, each color represents a different problem. Bottom: relative sub-optimality gap for each problem after 40 and 100 iterations.

Loss function. We build a loss function based on the final values $(f^d(x_K^d))_{d \in \{1, \dots, D\}}$. However, to avoid biasing the training process, we also make the loss function robust to shifts by using the sub-optimality gap $f^d(x_K^d) - f^{d,*}$ where $f^{d,*}$ is the minimum of f^d . A key element to take into account in optimization is that the magnitude of function values may heavily vary between problems and across iterations. This can be slightly mitigated by normalizing by the initial sub-optimality gap $f^d(x_0^d) - f^{d,*}$, however we instead propose to run vanilla BFGS for K iterations as well and normalize by its sub-optimality gap. After averaging over all problems our loss function is:

$$\mathcal{L}(\theta) = \frac{1}{D} \sum_{d=1}^D \log \left(1 + \frac{f^d(x_K^d(\theta)) - f^{d,*}}{f^d(\tilde{x}_K^d) - f^{d,*}} \right), \quad (5)$$

where \tilde{x}_K^d is the K -th iteration of BFGS applied to the same problem. Note that we additionally use a logarithmic transformation to make the loss even more robust to different magnitudes. We emphasize that the algorithm does not make use of $f^{d,*}$ which is only used for training.

Initialization of \mathcal{M} . Training L2O models is notoriously difficult as the loss function may easily explode [69]. Our approach allows for a specific trick that dramatically stabilizes training. Indeed, according to Section 4.1 BFGS is a special case of our algorithm in which $y_k = d_k$. By initializing the weights of the last FF layer to zero and the linear layer to be $(0, 0, 0, 0, 1, 0)$ one can check that our algorithm is initialized to exactly coincide with BFGS. According to (5), the initial value of the loss function is always $\log(2)$ which dramatically stabilizes the training as shown in Figure 6 in Appendix F. To the best of our knowledge this is a completely new approach.

Methodology and results. We construct a training set of $D = 20$ problems made of ill-conditioned quadratics functions in dimension $n = 100$ with eigenvalues generated at random and random initializations. The details are provided in Appendix E. We train our model for $K = 40$ iterations. We then evaluate the performance of the algorithm on several settings that differ from the training one: more than 40 iterations, in-distribution test problems, OOD ones, OOD quadratics in larger dimension and finally on logistic regression.

Looking first at the training setting in Figure 3, observe that our L2O model improves upon BFGS for every problem after 40 iterations, sometimes by several orders of magnitudes. This significant improvement transfers to 100 (trained only for 40) iterations for almost all problems, and also to the test set and most OOD problems. Testing the algorithm on quadratic functions in dimension 500 and logistic regression in Figure 4, observe that not only our model does not break but even improves upon vanilla BFGS in most cases despite not having been trained on such problems (although the

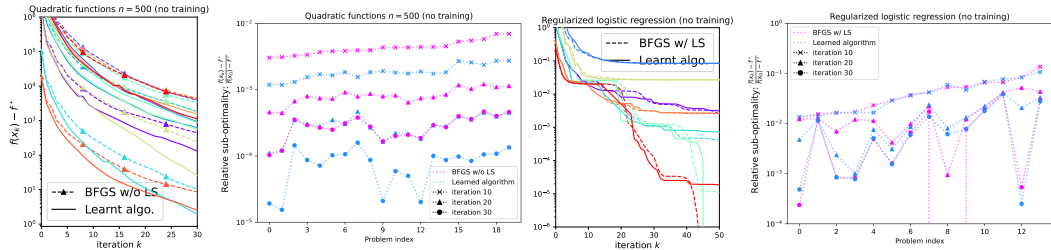


Figure 4: Sub-optimality gap against iterations on problems that are different from the training setting, each color represents a different problem. The two left plots are for quadratic functions dimension $n = 500$ and right plots show regularized logistic regression (see Appendix E). For the logistic regression problems, line-search is used both for BFGS and Algorithm 2.

improvement is not as dramatic as on the training set). These experiments evidence the benefits of the strategy proposed in Section 3 in order to achieve generalization (Section 2.2).

6 Related Work and Comparison

L2O [40] is a recent but active topic of research. A lot of work focuses on unrolling [26, 1, 31, 44] and «Plug and Play» [66, 48, 75, 64] approaches which improve over classical algorithms in several practical cases. L2O often lacks theoretical guarantees, with a few exceptions where convergence is enforced with “safeguards” [51, 28, 47], possibly discarding the model’s prediction, or estimated statistically [63], which does not apply OOD. The literature on L2O is broad, we refer to [16] for a detailed overview of the topic.

One of our contributions is to identify and enforce equivariance or invariance to transformations in L2O. In fact, in standard optimization [20] hypothesizes that these equivariances might be the reason for the success of BFGS (see below). Geometric deep learning [10] is a popular topic that studies these equivariances in the learning context, with many applications [60, 13, 33, 64, 14, 36, 39]. It is also connected to learning on sets [72, 38]. To the best of our knowledge the only work really discussing equivariances for L2O is [53], from a probabilistic point of view. Our work rather studies how to treat these properties in every step of a general L2O pipeline (through Algorithm 1). Recently, [45] also advocated for more mathematical structure in L2O, but rather proposed to enforce convergence properties by design, hence stabilizing L2O methods, whereas our principles aim to improve generalization. Improving the design of L2O algorithms has been studied in [70, 49, 50] and [15] also proposed to enhance algorithms and train by competing against a baseline, but not in relative function values as we do in (5).

The BFGS algorithm [11, 19, 24, 62] is the most popular QN algorithm. BFGS has been extensively analyzed [25, 18, 58] and many extensions have been proposed, featuring limited memory [43], sparse [65] and non-smooth [68] versions, or modifications provably faster in specific settings [59, 35]. Other approaches to make use of second-order derivatives only relying on gradients include symmetric-rank-one methods [17, 7] and the dynamical inertial Newton family of methods [2, 4, 5] which is at the interface of first-and second-order optimization [12].

Different approach have been proposed to learn BFGS methods. A transformer model has been derived by [22], and [42] considered learning on the fly in the online setting. The idea to combine the variational formulation from Section 4.1 with learning has been studied in [29] for Bayesian optimization. A recent work [41] predicted a weighted average between DFP [57] and BFGS (a.k.a. a Broyden method). This is more akin to hyper-parameter tuning as their method remains in the span of Broyden’s family. In contrast our method can construct possibly very different matrices $(B_k)_{k \in \mathbb{N}}$.

7 Conclusion

We provided a new approach to design more robust learned optimization algorithms. Our work blends all aspects of L2O: from optimization theory to machine learning models, including implementation and training considerations. Applying our techniques to build a L2O-enhanced BFGS algorithm

shows how promising the approach is in practice, and results in an algorithm outperforming vanilla BFGS consistently beyond the training setting. Enhancing existing algorithms allowed us to provide theoretical guarantees, which most L2O algorithms lack of, as well as a new training strategy that significantly eases the training and could mitigate the difficulty of training many L2O models. This work calls for exploring many directions such as designing more advanced models, enhancing other algorithms, adding new principles, considering stochastic algorithms and even combining our guarantees with statistical ones.

Acknowledgements

This work is supported by the ANR-DFG joint project TRINOM-DS under number DFG-OC150/5-1. C. Castera thanks Michael Sucker for useful discussions. We also thank the development teams of the following libraries: Python [61], Matplotlib [32] and Pytorch[54].

References

- [1] Pierre Ablin, Thomas Moreau, Mathurin Massias, and Alexandre Gramfort. Learning step sizes for unfolded sparse coding. In *Advances in Neural Information Processing Systems (NeurIPS)*, volume 32, 2019.
- [2] Felipe Alvarez, Hedy Attouch, Jérôme Bolte, and Patrick Redont. A second-order gradient-like dissipative dynamical system with Hessian-driven damping.: Application to optimization and mechanics. *Journal de mathématiques pures et appliquées*, 81(8):747–779, 2002.
- [3] Marcin Andrychowicz, Misha Denil, Sergio Gomez, Matthew W Hoffman, David Pfau, Tom Schaul, H. Brendan Shillingford, and Nando De Freitas. Learning to learn by gradient descent by gradient descent. In *Advances in Neural Information Processing Systems (NeurIPS)*, volume 29, 2016.
- [4] Hedy Attouch, Juan Peypouquet, and Patrick Redont. Fast convex optimization via inertial dynamics with Hessian driven damping. *Journal of Differential Equations*, 261(10):5734–5783, 2016.
- [5] Hedy Attouch, Zaki Chbani, Jalal Fadili, and Hassan Riahi. First-order optimization algorithms via inertial systems with Hessian driven damping. *Mathematical Programming*, pages 1–43, 2022.
- [6] Jonathan Barzilai and Jonathan M Borwein. Two-point step size gradient methods. *IMA journal of numerical analysis*, 8(1):141–148, 1988.
- [7] Stephen Becker and Jalal Fadili. A quasi-Newton proximal splitting method. In *Advances in Neural Information Processing Systems (NeurIPS)*, volume 25, 2012.
- [8] Stephen Becker, Jalal Fadili, and Peter Ochs. On quasi-Newton forward–backward splitting: Proximal calculus and convergence. *SIAM Journal on Optimization*, 29(4):2445–2481, 2019.
- [9] Dimitri P Bertsekas. Nonlinear programming. *Journal of the Operational Research Society*, 48(3):334–334, 1997.
- [10] Michael M Bronstein, Joan Bruna, Taco Cohen, and Petar Veličković. Geometric deep learning: Grids, groups, graphs, geodesics, and gauges. *arXiv preprint arXiv:2104.13478*, 2021.
- [11] Charles George Broyden. The convergence of a class of double-rank minimization algorithms. *IMA Journal of Applied Mathematics*, 6(1):76–90, 1970.
- [12] Camille Castera, Hedy Attouch, Jalal Fadili, and Peter Ochs. Continuous Newton-like methods featuring inertia and variable mass. *SIAM Journal on Optimization*, 34(1):251–277, 2024.
- [13] Dongdong Chen, Julián Tachella, and Mike E Davies. Equivariant imaging: Learning beyond the range space. In *International Conference on Computer Vision (ICCV)*, pages 4379–4388, 2021.

- [14] Dongdong Chen, Mike Davies, Matthias J Ehrhardt, Carola-Bibiane Schönlieb, Ferdia Sherry, and Julián Tachella. Imaging with equivariant deep learning: From unrolled network design to fully unsupervised learning. *IEEE Signal Processing Magazine*, 40(1):134–147, 2023.
- [15] Tianlong Chen, Weiyi Zhang, Zhou Jingyang, Shiyu Chang, Sijia Liu, Lisa Amini, and Zhangyang Wang. Training stronger baselines for learning to optimize. In *Advances in Neural Information Processing Systems (NeurIPS)*, volume 33, pages 7332–7343, 2020.
- [16] Tianlong Chen, Xiaohan Chen, Wuyang Chen, Howard Heaton, Jialin Liu, Zhangyang Wang, and Wotao Yin. Learning to optimize: A primer and a benchmark. *Journal of Machine Learning Research*, 23(189):1–59, 2022.
- [17] Andrew R Conn, Nicholas IM Gould, and Philippe L Toint. Convergence of quasi-Newton matrices generated by the symmetric rank one update. *Mathematical programming*, 50(1): 177–195, 1991.
- [18] John E Dennis, Jr and Jorge J Moré. Quasi-Newton methods, motivation and theory. *SIAM review*, 19(1):46–89, 1977.
- [19] Roger Fletcher. A new approach to variable metric algorithms. *The computer journal*, 13(3): 317–322, 1970.
- [20] Roger Fletcher. Newton-like methods. In *Practical Methods of Optimization*, chapter 3, pages 44–79. John Wiley & Sons, Ltd, 2000.
- [21] Guillaume Garrigos and Robert M Gower. Handbook of convergence theorems for (stochastic) gradient methods. *arXiv preprint arXiv:2301.11235*, 2023.
- [22] Erik Gärtner, Luke Metz, Mykhaylo Andriluka, C Daniel Freeman, and Cristian Sminchisescu. Transformer-based learned optimization. In *Conference on Computer Vision and Pattern Recognition (CVPR)*, pages 11970–11979, 2023.
- [23] Euhanna Ghadimi, Hamid Reza Feyzmahdavian, and Mikael Johansson. Global convergence of the heavy-ball method for convex optimization. In *European Control Conference (ECC)*, pages 310–315. IEEE, 2015.
- [24] Donald Goldfarb. A family of variable-metric methods derived by variational means. *Mathematics of computation*, 24(109):23–26, 1970.
- [25] John Greenstadt. Variations on variable-metric methods. *Mathematics of Computation*, 24(109): 1–22, 1970.
- [26] Karol Gregor and Yann LeCun. Learning fast approximations of sparse coding. In *International Conference on Machine Learning (ICML)*, pages 399–406, 2010.
- [27] Trevor Hastie, Robert Tibshirani, Jerome H Friedman, and Jerome H Friedman. *The elements of statistical learning: data mining, inference, and prediction*, volume 2. Springer, 2009.
- [28] Howard Heaton, Xiaohan Chen, Zhangyang Wang, and Wotao Yin. Safeguarded learned convex optimization. In *Proceedings of the AAAI Conference on Artificial Intelligence*, volume 37, pages 7848–7855, 2023.
- [29] Philipp Hennig and Martin Kiefel. Quasi-Newton methods: A new direction. *Journal of Machine Learning Research*, 14(1):843–865, 2013.
- [30] Sepp Hochreiter and Jürgen Schmidhuber. Long short-term memory. *Neural computation*, 9(8): 1735–1780, 1997.
- [31] Yunshi Huang, Emilie Chouzenoux, and Jean-Christophe Pesquet. Unrolled variational bayesian algorithm for image blind deconvolution. *IEEE Transactions on Image Processing*, 32:430–445, 2022.
- [32] John D Hunter. Matplotlib: A 2D graphics environment. *Computing in science & engineering*, 9(3):90–95, 2007.

- [33] Michael J Hutchinson, Charline Le Lan, Sheheryar Zaidi, Emilien Dupont, Yee Whye Teh, and Hyunjik Kim. Lietransformer: Equivariant self-attention for lie groups. In *International Conference on Machine Learning (ICML)*, pages 4533–4543, 2021.
- [34] Samy Jelassi and Yuanzhi Li. Towards understanding how momentum improves generalization in deep learning. In *International Conference on Machine Learning (ICML)*, pages 9965–10040, 2022.
- [35] Qiujiang Jin, Alec Koppel, Ketan Rajawat, and Aryan Mokhtari. Sharpened quasi-Newton methods: Faster superlinear rate and larger local convergence neighborhood. In *International Conference on Machine Learning (ICML)*, pages 10228–10250, 2022.
- [36] Nicolas Keriven and Samuel Vaiter. What functions can graph neural networks compute on random graphs? the role of positional encoding. In *Advances in Neural Information Processing Systems (NeurIPS)*, volume 36, 2024.
- [37] Diederik P. Kingma and Jimmy Ba. Adam: A method for stochastic optimization. In *International Conference on Learning Representations (ICLR)*, 2015.
- [38] Juho Lee, Yoonho Lee, Jungtaek Kim, Adam Kosiorek, Seungjin Choi, and Yee Whye Teh. Set transformer: A framework for attention-based permutation-invariant neural networks. In *International Conference on Machine Learning (ICML)*, pages 3744–3753, 2019.
- [39] Eitan Levin and Mateo Díaz. Any-dimensional equivariant neural networks. In *International Conference on Artificial Intelligence and Statistics (AISTAT)*, pages 2773–2781, 2024.
- [40] Ke Li and Jitendra Malik. Learning to optimize. In *International Conference on Learning Representations (ICLR)*, volume 4, 2016.
- [41] Maojia Li, Jialin Liu, and Wotao Yin. Learning to combine quasi-Newton methods. *arXiv preprint arXiv:2210.06171*, 2023.
- [42] Isaac Liao, Rumen Dangovski, Jakob Nicolaus Foerster, and Marin Soljagic. Learning to optimize quasi-Newton methods. *Transactions on Machine Learning Research*, 2023.
- [43] Dong C Liu and Jorge Nocedal. On the limited memory BFGS method for large scale optimization. *Mathematical programming*, 45(1):503–528, 1989.
- [44] Jialin Liu and Xiaohan Chen. ALISTA: Analytic weights are as good as learned weights in LISTA. In *International Conference on Learning Representations (ICLR)*, 2019.
- [45] Jialin Liu, Xiaohan Chen, Zhangyang Wang, Wotao Yin, and HanQin Cai. Towards constituting mathematical structures for learning to optimize. In *International Conference on Machine Learning (ICML)*, pages 21426–21449, 2023.
- [46] James Martens and Roger Grosse. Optimizing neural networks with Kronecker-factored approximate curvature. In *International Conference on Machine Learning (ICML)*, pages 2408–2417, 2015.
- [47] Andrea Martin and Luca Furieri. Learning to optimize with convergence guarantees using nonlinear system theory. *arXiv preprint arXiv:2403.09389*, 2024.
- [48] Tim Meinhardt, Michael Moller, Caner Hazirbas, and Daniel Cremers. Learning proximal operators: Using denoising networks for regularizing inverse imaging problems. In *International Conference on Computer Vision (ICCV)*, pages 1781–1790, 2017.
- [49] Luke Metz, Niru Maheswaranathan, Jeremy Nixon, Daniel Freeman, and Jascha Sohl-Dickstein. Understanding and correcting pathologies in the training of learned optimizers. In *International Conference on Machine Learning (ICML)*, pages 4556–4565, 2019.
- [50] Luke Metz, C Daniel Freeman, James Harrison, Niru Maheswaranathan, and Jascha Sohl-Dickstein. Practical tradeoffs between memory, compute, and performance in learned optimizers. In *Conference on Lifelong Learning Agents*, pages 142–164, 2022.

- [51] Michael Moeller, Thomas Mollenhoff, and Daniel Cremers. Controlling neural networks via energy dissipation. In *International Conference on Computer Vision (ICCV)*, pages 3256–3265, 2019.
- [52] Yurii Nesterov et al. *Lectures on convex optimization*, volume 137. Springer, 2018.
- [53] Yann Ollivier, Ludovic Arnold, Anne Auger, and Nikolaus Hansen. Information-geometric optimization algorithms: A unifying picture via invariance principles. *Journal of Machine Learning Research*, 18(18):1–65, 2017.
- [54] Adam Paszke, Sam Gross, Francisco Massa, Adam Lerer, James Bradbury, Gregory Chanan, Trevor Killeen, Zeming Lin, Natalia Gimelshein, Luca Antiga, et al. Pytorch: An imperative style, high-performance deep learning library. In *Advances in Neural Information Processing Systems (NeurIPS)*, volume 32, 2019.
- [55] Boris T Polyak. Some methods of speeding up the convergence of iteration methods. *USSR Computational Mathematics and Mathematical Physics*, 4(5):1–17, 1964.
- [56] Boris T Polyak. *Introduction to optimization*. New York, Optimization Software., 1987.
- [57] Michael JD Powell. Variable metric methods for constrained optimization. *Mathematical Programming The State of the Art: Bonn 1982*, pages 288–311, 1983.
- [58] Ge Ren-Pu and Michael JD Powell. The convergence of variable metric matrices in unconstrained optimization. *Mathematical programming*, 27:123–143, 1983.
- [59] Anton Rodomanov and Yurii Nesterov. Greedy quasi-Newton methods with explicit superlinear convergence. *SIAM Journal on Optimization*, 31(1):785–811, 2021.
- [60] David W Romero and Jean-Baptiste Cordonnier. Group equivariant stand-alone self-attention for vision. In *International Conference on Learning Representations (ICLR)*, 2020.
- [61] Guido Rossum. *Python reference manual*. CWI (Centre for Mathematics and Computer Science), 1995.
- [62] David F Shanno. Conditioning of quasi-Newton methods for function minimization. *Mathematics of computation*, 24(111):647–656, 1970.
- [63] Michael Sucker and Peter Ochs. PAC-Bayesian learning of optimization algorithms. In *International Conference on Artificial Intelligence and Statistics (AISTAT)*, pages 8145–8164, 2023.
- [64] Matthieu Terris, Thomas Moreau, Nelly Pustelnik, and Julian Tachella. Equivariant plug-and-play image reconstruction. *arXiv preprint arXiv:2312.01831*, 2023.
- [65] Philippe L Toint. A sparse quasi-Newton update derived variationally with a nondiagonally weighted Frobenius norm. *mathematics of computation*, 37(156):425–433, 1981.
- [66] Singanallur V Venkatakrisnan, Charles A Bouman, and Brendt Wohlberg. Plug-and-play priors for model based reconstruction. In *2013 IEEE global conference on signal and information processing*, pages 945–948. IEEE, 2013.
- [67] Stéfan van der Walt, Chris Colbert, and Gael Varoquaux. The NumPy array: a structure for efficient numerical computation. *Computing in Science & Engineering*, 13(2):22–30, 2011.
- [68] Shida Wang, Jalal Fadili, and Peter Ochs. Inertial quasi-Newton methods for monotone inclusion: efficient resolvent calculus and primal-dual methods. *arXiv preprint arXiv:2209.14019*, 2022.
- [69] Xiang Wang, Shuai Yuan, Chenwei Wu, and Rong Ge. Guarantees for tuning the step size using a learning-to-learn approach. In *International Conference on Machine Learning (ICML)*, pages 10981–10990, 2021.
- [70] Olga Wichrowska, Niru Maheswaranathan, Matthew W Hoffman, Sergio Gomez Colmenarejo, Misha Denil, Nando Freitas, and Jascha Sohl-Dickstein. Learned optimizers that scale and generalize. In *International Conference on Machine Learning (ICML)*, pages 3751–3760, 2017.

- [71] David H Wolpert. The lack of a priori distinctions between learning algorithms. *Neural computation*, 8(7):1341–1390, 1996.
- [72] Manzil Zaheer, Satwik Kottur, Siamak Ravanbakhsh, Barnabas Poczos, Russ R Salakhutdinov, and Alexander J Smola. Deep sets. In *Advances in Neural Information Processing Systems (NeurIPS)*, volume 30, 2017.
- [73] SK Zavriev and FV Kostyuk. Heavy-ball method in nonconvex optimization problems. *Computational Mathematics and Modeling*, 4(4):336–341, 1993.
- [74] Chiyuan Zhang, Samy Bengio, Moritz Hardt, Benjamin Recht, and Oriol Vinyals. Understanding deep learning (still) requires rethinking generalization. *Communications of the ACM*, 64(3): 107–115, 2021.
- [75] Kai Zhang, Yawei Li, Wangmeng Zuo, Lei Zhang, Luc Van Gool, and Radu Timofte. Plug-and-play image restoration with deep denoiser prior. *IEEE Transactions on Pattern Analysis and Machine Intelligence*, 44(10):6360–6376, 2021.

A Detailed Analysis of Equivariance and Invariance of Popular Algorithms

Below we detail how to obtain the properties listed in Table 1. We begin by studying the transformations.

A.1 The Chain-rule

In this section we detail how each transformation affects the derivatives of f . All these results are based on the chain-rule. For an invertible mapping $\mathcal{T}: \mathbb{R}^n \rightarrow \mathbb{R}^n$, we study the function $\hat{f} = f \circ \mathcal{T}^{-1}$. The chain rule states that $\forall y \in \mathbb{R}^n$

$$D_y(\hat{f}) = D_y(f \circ \mathcal{T}^{-1}) = D_{\mathcal{T}^{-1}(y)}(f) \cdot D_y(\mathcal{T}^{-1}),$$

where $D_y \hat{f}$ is the Jacobian of \hat{f} at y . Rewriting this in terms of gradients (the transpose of the Jacobian):

$$\nabla \hat{f}(y) = (D_y(\mathcal{T}^{-1}))^T \nabla f(\mathcal{T}^{-1}(y)).$$

In most of what follows we will apply the chain rule above to the point $\hat{x} = \mathcal{T}(x)$, which yields

$$\nabla \hat{f}(\hat{x}) = (D_{\mathcal{T}(x)}(\mathcal{T}^{-1}))^T \nabla f(\mathcal{T}^{-1}(\mathcal{T}(x))) = (D_{\mathcal{T}(x)}(\mathcal{T}^{-1}))^T \nabla f(x),$$

so the Jacobian of \mathcal{T}^{-1} captures how the gradient is transformed. We now detail this for each transformation.

A.2 List of Transformations

We consider the transformations in Table 1. For each case we redefine \mathcal{T} and, without restating it, define $\hat{f} = f \circ \mathcal{T}^{-1}$ and $\hat{x} = \mathcal{T}(x)$, for all $x \in \mathbb{R}^n$.

Translation. Let $v \in \mathbb{R}^n$ and for all $x \in \mathbb{R}^n$, consider the translation $\mathcal{T}(x) = x + v$. Then one can see that $D(\mathcal{T}^{-1}) = \mathbb{I}_n$ which implies that $(D_{\mathcal{T}(x)}(\mathcal{T}^{-1}))^T = \mathbb{I}_n$. So, $\nabla \hat{f}(\hat{x}) = \nabla f(x)$ and similarly, one can show that $\nabla^2 \hat{f}(\hat{x}) = \nabla^2 f(x)$.

Orthogonal Linear Transformations. Let $P \in \mathbb{R}^{n \times n}$ an orthogonal matrix ($P^T P = \mathbb{I}_n$) and $\mathcal{T}: x \in \mathbb{R}^n \mapsto Px$. Then using the orthogonality of P , $\mathcal{T}^{-1}(x) = P^{-1}x = P^T x$. It is a linear mapping, so $D\mathcal{T}^{-1} = P^T$ and $(D_{\mathcal{T}(x)}(\mathcal{T}^{-1}))^T = (P^T)^T = P$. Therefore $\nabla \hat{f}(\hat{x}) = P \nabla f(x)$. Similarly, using the linearity of \mathcal{T}^{-1} , we can show that $\nabla^2 \hat{f}(\hat{x}) = P \nabla^2 f(x) P^T$.

Permutations. Permutation matrices are a specific type of orthogonal matrices, therefore the above directly applies.

Geometric Rescaling. Let $\lambda > 0$ and consider the transformation $\mathcal{T}: x \in \mathbb{R}^n \mapsto \lambda x$. Then $\mathcal{T}^{-1}(x) = \frac{1}{\lambda}x$ which is again a linear mapping so $D\mathcal{T}^{-1} = \frac{1}{\lambda}\mathbb{I}_n$. We deduce as before that $\nabla \hat{f}(\hat{x}) = \frac{1}{\lambda}\nabla f(x)$ and $\nabla^2 \hat{f}(\hat{x}) = \frac{1}{\lambda^2}\nabla^2 f(x)$.

Function Rescaling. Let $\lambda > 0$, when considering $\hat{f} = \lambda f$, the linearity of the differentiation directly gives $\nabla \hat{f} = \lambda \nabla f$ and $\nabla^2 \hat{f} = \lambda \nabla^2 f$.

A.3 Analysis of Popular Algorithms

We now show the properties of Table 1 for each algorithm therein, except BFGS which is analyzed together with Algorithm 2 later in Section B. Each time, the proofs are done by induction. We can safely assume that x_0 and S_0 are properly adapted so that the induction holds for $k = 0$ (this was explained in Section 3).

To show each equivariance property (or invariance in the case of function rescaling), we fix $k \in \mathbb{N}$ and assume that the equivariance holds for all iterates up to k , and then prove that it still holds at iteration $k + 1$.

Gradient descent and HB. We already extensively discussed the properties of HB which was our running example in Section 3.1. As for gradient descent, it is simply HB with $\alpha = 0$. Using the results of Section A.2 one can straightforwardly deduce translation, permutations and orthogonal equivariances. Thus we only discuss the case of rescaling. For $\lambda > 0$ and $\hat{f} = f(\frac{1}{\lambda} \cdot)$, assuming that the induction hypothesis $\hat{x}_k = \lambda x_k$ holds, we previously showed that, $\nabla \hat{f}(\hat{x}_k) = \frac{1}{\lambda} \nabla f(x_k)$, so the iteration of HB reads,

$$\hat{x}_{k+1} = \hat{x}_k + \alpha \hat{d}_k + \gamma \nabla \hat{f}(\hat{x}_k) = \lambda x_k + \lambda \alpha d_k + \frac{\gamma}{\lambda} \nabla f(x_k).$$

So for $\lambda \neq 1$ we see that $\hat{x}_{k+1} \neq \lambda x_{k+1}$. This can be fixed however by tuning γ specifically for each problem (we would get $\hat{\gamma} = \lambda^2 \gamma$). The case of function rescaling $\hat{f} = \lambda f$ is almost identical.

Newton's method. The update of Newton's method reads

$$x_{k+1} = x_k - [\nabla^2 f(x_k)]^{-1} \nabla f(x_k).$$

As above, translation equivariance is straightforward. As for orthogonal matrices P , using the results from Section A.2 it holds that

$$\begin{aligned} \hat{x}_{k+1} &= \hat{x}_k - [\nabla^2 \hat{f}(\hat{x}_k)]^{-1} \nabla \hat{f}(\hat{x}_k) = Px_k - [P \nabla^2 f(x_k) P^T]^{-1} P \nabla f(x_k) \\ &= Px_k - (P^T)^{-1} [\nabla^2 f(x_k)]^{-1} P^{-1} P \nabla f(x_k) = Px_k - P [\nabla^2 f(x_k)]^{-1} \nabla f(x_k), \end{aligned}$$

which proves the equivariance.

For geometric rescaling by $\lambda > 0$, remark from Section A.2 that the inverse Hessian is rescaled by λ^2 and the gradient is rescaled by $1/\lambda$, so the result follows. The same is true for invariance with respect to function rescaling.

The ADAM Algorithm. The iterations of the ADAM algorithm read

$$\begin{cases} m_k &= \beta_1 m_{k-1} + (1 - \beta_1) \nabla f(x_k) \\ v_k^2 &= \beta_2 v_{k-1}^2 + (1 - \beta_2) \nabla f(x_k) \odot \nabla f(x_k), \\ x_{k+1} &= x_k - \frac{m_k}{\sqrt{v_k^2}} \end{cases}$$

where $\beta_1, \beta_2 \in [0, 1)$, \odot denotes the element-wise product, the square root and quotient are applied element wise, and $m_{-1}, v_{-1}^2 \in \mathbb{R}^n$.

Again, translation equivariance is straightforward using the results from section A.2. The robustness with respect to the two scalings is also easy to check in that case since both m_k and $\sqrt{v_k^2}$ are rescaled like ∇f . We now consider an orthogonal matrix P . According to section A.2 and assuming that up to iteration k ADAM is equivariant to orthogonal transformations, we have $\hat{f}(\hat{x}) = P \nabla f(x)$ and $\hat{m}_k = P m_k$. However, looking at v_k^2 , note that

$$\nabla \hat{f}(\hat{x}_k) \odot \nabla \hat{f}(\hat{x}_k) = (P \nabla f(x_k)) \odot (P \nabla f(x_k)) \quad (6)$$

which in general is not equal to $P(\nabla f(x_k) \odot \nabla f(x_k))$. Therefore, for most orthogonal matrices we do not have $\hat{v}_k = P v_k$ and equivariance does not hold.

Nevertheless, in the special case where P is a permutation matrix, each line of P contains exactly one coefficient equal to one and all others are zero. Since \odot is an element-wise operation, one can check that we then have $(P\nabla f(x_k)) \odot (P\nabla f(x_k)) = P(\nabla f(x_k) \odot \nabla f(x_k))$ such that $\hat{v}_k = Pv_k$. Applying the same reasoning to all other element-wise operations in (6), we deduce that, despite not being equivariant to all orthogonal matrices, ADAM is permutation equivariant.

A.4 On the Difficulty of Preserving Orthogonal Equivariance for LOA

The discussion above regarding ADAM shows why preserving equivariance to all orthogonal matrices is very hard for LOA since even element-wise operation may not commute with orthogonal matrices.

To give an example, let P an orthogonal matrix, let $y \in \mathbb{R}^n$ and $\sigma: \mathbb{R} \rightarrow \mathbb{R}$ be a *non-linear* activation function (to be applied element wise in layers of a neural network). To preserve equivariance with respect to P , one would want that $\sigma(Py) = P\sigma(y)$, which, for the i -th coordinate reads,

$$\sigma\left(\sum_{j=1}^n P_{i,j}y_j\right) = \sum_{j=1}^n P_{i,j}\sigma(y)_j. \quad (7)$$

Yet, since σ is assumed to be non-linear, it does not commute with the sum (which would still not be sufficient for (7) to hold). Therefore, if y is the result of an FF layer (used coordinate-wise like in Algorithm 2) in a neural network, then applying a non-linear activation function (e.g., ReLU or sigmoid), we see that equivariance with respect to P is broken. This shows that orthogonal equivariance is not even compatible with coordinate-wise FF layers and hence hardly possible to achieve for LOA.

Finally, note that when P is a permutation matrix, then $\forall i \in \{1, \dots, n\}$, there exists $l \in \{1, \dots, n\}$ such that $P_{i,l} = 1$ and for all $j \neq l$, $P_{i,j} = 0$. So (7) becomes

$$\sigma(P_{i,l}y_l) = P_{i,l}\sigma(y)_l \iff \sigma(y_l) = \sigma(y)_l, \quad (8)$$

and since σ is applied element wise, (8) holds true. So permutation equivariance is more compatible with LOA than orthogonal equivariance.

B Proof of Theorem 1

Proof of Theorem 1. Principle 1 holds by construction of the algorithm where n is not used to choose p nor n_i . We now prove that Principles 2 to 5 hold one by one. As for other algorithms in Section A.3, in each case we explicitly state which transformation \mathcal{T} is considered and implicitly redefine $\hat{f} = f \circ \mathcal{T}^{-1}$ and define $(\hat{x}_k)_{k \in \mathbb{N}}$ as the iterates of the algorithm applied to $(\hat{f}, \hat{x}_0, \hat{S}_0)$ (all quantities with a “hat” symbol are defined accordingly). We again proceed by induction: we fix $k \in \mathbb{N}$ and assume that equivariance (or invariance for Principle 5) holds up to iteration k and show that it still holds at iteration $k + 1$. We also show that the principles hold at $k = 0$ by construction.

Unlike the algorithms discussed in Section A.3, Algorithm 2 and BFGS additionally use a matrix B_k , (stored in the state S_{k+1}). Since B_k aims to approximate the inverse Hessian $\nabla^2 f(x_k)^{-1}$, we expect B_k to be transformed by \mathcal{T} in the same way as $\nabla^2 f(x_k)^{-1}$ is (see Section A.2). We will prove that this is the case, again by induction.

Translation. Let $v \in \mathbb{R}^n$ and the translation $\mathcal{T}: x \in \mathbb{R}^n \mapsto x + v$. Assume that $\forall i \leq k$, $\hat{x}_i = \mathcal{T}(x_i) = x_i + v$ and that $\forall i \leq k - 1$, $\hat{B}_i = B_i$. Then $\hat{d}_k = \hat{x}_k - \hat{x}_{k-1} = d_k$ and we showed in Section A.2 that $\nabla \hat{f}(\hat{x}_k) = \nabla f(x_k)$. Similarly, $\widehat{\Delta g}_k = \Delta g_k$. So,

$$\hat{I}_k = \left(\hat{B}_{k-1} \widehat{\Delta g}_k, \hat{d}_k, -\gamma \hat{B}_{k-1} \nabla \hat{f}(\hat{x}_k) \right) = (B_{k-1} \Delta g_k, d_k, -\gamma B_{k-1} \nabla f(x_k)) = I_k,$$

This is not surprising as we explained in Section 3.1 that we constructed \mathcal{C} so that the above is true. Then we directly deduce $\hat{y}_k = \mathcal{M}(\hat{I}_k, \theta) = \mathcal{M}(I_k, \theta) = y_k$ and the rest of the proof follows.

As for the case $k = 0$, by construction (see Section 3), $\hat{x}_0 = x_0 + v$ and $\hat{x}_{-1} = x_{-1} + v$. One can then easily check that our choice of B_{-1} (defined in Section 4.2) is translation invariant. So by induction, Principle 2 holds.

Permutation. Let P and permutation matrix of \mathbb{R}^n and let $\mathcal{T}: x \in \mathbb{R}^n \mapsto Px$. Assume that $\forall i \leq k$, $\hat{x}_i = \mathcal{T}(x_i) = Px_i$ and that $\forall i \leq k-1$, $\hat{B}_i = PB_iP^T$. Note that the hypothesis on B_i matches that of the inverse Hessian in Section A.2. Then $\hat{d}_k = Px_k - Px_{k-1} = Pd_k$. We showed in Section A.2 that $\nabla \hat{f}(\hat{x}_k) = P\nabla f(x_k)$, and similarly, $\widehat{\Delta}g_k = P\Delta g_k$. So,

$$\hat{I}_k = (PB_{k-1}P^T P\Delta g_k, Pd_k, -\gamma PB_{k-1}P^T P\nabla f(x_k)) = PI_k,$$

i.e., \mathcal{C} is permutation equivariant as intended. Then $\hat{y}_k = \mathcal{M}(\hat{I}_k, \theta) = \mathcal{M}(PI_k, \theta)$ and as justified in Appendix A.4, all the operations applied element-wise in \mathcal{M} are permutation equivariant, and the averaging also is. So \mathcal{M} is permutation equivariant, *i.e.*, $\hat{y}_k = Py_k$.

Regarding the step \mathcal{U} , we recall the notation $r_k = d_k - B_{k-1}\Delta g_k$ used in (4). Remark that $\hat{r}_k = Pd_k - PB_{k-1}\Delta g_k = Pr_k$, and substituting \hat{y}_k , $\widehat{\Delta}g_k$ and \hat{r}_k in (4) (and using again $P^T P = \mathbb{I}_n$), we obtain $\hat{B}_k = PB_kP^T$ and $\hat{x}_{k+1} = Px_{k+1}$.

Finally, at $k = 0$, by construction $\hat{x}_0 = Px_0$ and $\hat{x}_{-1} = Px_{-1}$ and one can easily check that $\hat{\gamma}_{\text{BB}}^{(0)} = \gamma_{\text{BB}}^{(0)}$ (again due to P being orthogonal), such that $\hat{B}_{-1} = B_{-1}$. So Principle 3 holds true.

Geometric rescaling. Let $\lambda > 0$ and let $\mathcal{T}: x \in \mathbb{R}^n \mapsto \lambda x$. Assume that $\forall i \leq k$, $\hat{x}_i = \mathcal{T}(x_i) = \lambda x_i$ and that $\forall i \leq k-1$, $\hat{B}_i = \lambda^2 B_i$ (as in Section A.2). Then $\hat{d}_k = \lambda x_k - \lambda x_{k-1} = \lambda d_k$. We also showed in Section A.2 that $\nabla \hat{f}(\hat{x}_k) = \frac{1}{\lambda} \nabla f(x_k)$, thus $\widehat{\Delta}g_k = \frac{1}{\lambda} \Delta g_k$. So,

$$\hat{I}_k = \left(\lambda^2 B_{k-1} \frac{\lambda^2}{\lambda} \Delta g_k, \lambda d_k, -\gamma \lambda^2 B_{k-1} \frac{\lambda^2}{\lambda} \nabla f(x_k) \right) = \lambda I_k,$$

which means that \mathcal{C} is equivariant as we prescribed. Then our model \mathcal{M} is a composition of linear operations and ReLU activation functions which are all equivariant to rescaling, so the model is equivariant, *i.e.*, $\hat{y}_k = \lambda y_k$. Plugging this into the update step we obtain

$$\hat{B}_k = \lambda^2 B_{k-1} + \frac{1}{\langle \lambda^{-1} \Delta g_k, \lambda y_k \rangle} \left[\lambda^2 r_k y_k^T + \lambda^2 y_k r_k^T - \frac{\langle \lambda^{-1} \Delta g_k, \lambda r_k \rangle}{\langle \lambda^{-1} \Delta g_k, \lambda y_k \rangle} \lambda^2 y_k y_k^T \right] = \lambda^2 B_k.$$

Finally, the case $k = 0$ holds by construction and thanks to the BB step-size since

$$\hat{\gamma}_{\text{BB}}^{(0)} = \frac{\langle \lambda^{-1} \Delta g_0, \lambda d_0 \rangle}{\lambda^{-2} \|\Delta g_0\|^2} = \lambda^2 \gamma_{\text{BB}}^{(0)}.$$

This shows how the choice of B_{-1} is crucial to preserve equivariance to rescaling. Overall Principle 4 holds.

Function rescaling. Let $\lambda > 0$ and consider $\hat{f} = \lambda f$. For this last principle we want to prove invariance of the algorithm. Therefore assume that $\forall i \leq k$, $\hat{x}_i = x_i$ and that $\forall i \leq k-1$, $\hat{B}_i = \frac{1}{\lambda} B_i$ (it scales like the inverse Hessian). Then $\hat{d}_k = d_k$ and we also have $\nabla \hat{f}(\hat{x}_k) = \lambda \nabla f(x_k)$, thus $\widehat{\Delta}g_k = \lambda \Delta g_k$. So

$$\hat{I}_k = \left(\frac{1}{\lambda} B_{k-1} \lambda \Delta g_k, d_k, -\gamma \frac{1}{\lambda} B_{k-1} \lambda \nabla f(x_k) \right) = I_k,$$

so \mathcal{C} is invariant, which directly implies $\hat{y}_k = y_k$ and then

$$\hat{B}_k = \frac{1}{\lambda} B_{k-1} + \frac{1}{\langle \lambda \Delta g_k, y_k \rangle} \left[r_k y_k^T + y_k r_k^T - \frac{\langle \lambda \Delta g_k, r_k \rangle}{\langle \lambda \Delta g_k, y_k \rangle} y_k y_k^T \right] = \frac{1}{\lambda} B_k.$$

Finally, the case $k = 0$ holds again thanks to the use of the BB step-size to initialize B_{-1} , which proves that Principle 5 holds and concludes the proof. \square

Remark 1. *The proof above can easily be applied to BFGS since it corresponds to the special case where \mathcal{M} is replaced by $y_k = d_k$.*

C Proof of Theorem 2

Proof of Theorem 2. Assume that f has L -Lipschitz continuous gradient, that is, for all $x, y \in \mathbb{R}^n$,

$$\|\nabla f(x) - \nabla f(y)\| \leq L \|x - y\|.$$

Then the *descent lemma* (see e.g., [21]) states that for all $x, y \in \mathbb{R}^n$,

$$f(y) \leq f(x) + \langle \nabla f(x), y - x \rangle + \frac{L}{2} \|y - x\|^2. \quad (9)$$

Now let $(x_k)_{k \in \mathbb{N}}$ and $(B_k)_{k \in \mathbb{N}}$ be respectively the sequence of iterates and the matrices generated by Algorithm 2 applied to (f, x_0, S_0) . Using the descent lemma (9), we get,

$$f(x_{k+1}) \leq f(x_k) + \langle \nabla f(x_k), -\gamma B_k \nabla f(x_k) \rangle + \frac{L}{2} \gamma^2 \|B_k \nabla f(x_k)\|^2,$$

which we rewrite

$$f(x_{k+1}) \leq f(x_k) + \left\langle B_k \nabla f(x_k), -\gamma \nabla f(x_k) + \frac{L}{2} \gamma^2 B_k \nabla f(x_k) \right\rangle. \quad (10)$$

By construction, (see (4)), B_k is real symmetric, so there exists an orthogonal matrix $P_k \in \mathbb{R}^{n \times n}$ and a diagonal matrix $D_k \in \mathbb{R}^{n \times n}$ such that,

$$B_k = P_k D_k P_k^T.$$

Using this in (10), we obtain

$$f(x_{k+1}) \leq f(x_k) + \left\langle P_k D_k P_k^T \nabla f(x_k), -\gamma P_k P_k^T \nabla f(x_k) + \frac{L}{2} \gamma^2 P_k D_k P_k^T \nabla f(x_k) \right\rangle,$$

where we used the fact that $P_k P_k^T = \mathbb{I}_n$ to write $\nabla f(x_k) = P_k P_k^T \nabla f(x_k)$. We denote $g_k = P_k^T \nabla f(x_k)$ and get:

$$\begin{aligned} f(x_{k+1}) &\leq f(x_k) + \left\langle P_k D_k g_k, -\gamma P_k g_k + \frac{L}{2} \gamma^2 P_k D_k g_k \right\rangle \\ &\iff f(x_{k+1}) \leq f(x_k) + \left\langle D_k g_k, -\gamma g_k + \frac{L}{2} \gamma^2 D_k g_k \right\rangle, \end{aligned} \quad (11)$$

where we used the fact that P_k is orthogonal in the last line. Since D_k is orthogonal, denoting by $(g_{k,i})_{i \in \{1, \dots, n\}}$ and $(b_{k,i})_{i \in \{1, \dots, n\}}$ the coordinates of g_k and the eigenvalues of B_k , respectively, we deduce that

$$\begin{aligned} \left\langle D_k g_k, -\gamma g_k + \frac{L}{2} \gamma^2 D_k g_k \right\rangle &= \sum_{i=1}^n b_{k,i} g_{k,i}^2 \left(-\gamma + \frac{L}{2} \gamma^2 b_{k,i} \right) = \gamma \sum_{i=1}^n b_{k,i} g_{k,i}^2 \left(\frac{L}{2} \gamma b_{k,i} - 1 \right) \\ &\leq \gamma \sum_{i=1}^n b_{k,i} g_{k,i}^2 \underbrace{\left(\frac{L}{2} \gamma C - 1 \right)}_{\leq 0} \leq 0, \end{aligned}$$

where for the last line we used the assumption that for all $k \in \mathbb{N}$ and $\forall i \in \{1, \dots, n\}$, $0 < b_{k,i} \leq C$ and that $\gamma \leq \frac{2}{CL}$. We use this in (11):

$$f(x_{k+1}) \leq f(x_k) - \gamma \left(1 - \frac{L}{2} \gamma C \right) \sum_{i=1}^n b_{k,i} g_{k,i}^2 \leq f(x_k). \quad (12)$$

So the sequence $(f(x_k))_{k \in \mathbb{N}}$ is non-increasing, and since f is a lower-bounded function, then $(f(x_k))_{k \in \mathbb{N}}$ converges.

We now sum (12) from $k = 0$ to $K \in \mathbb{N}$,

$$\begin{aligned} \sum_{k=0}^K f(x_{k+1}) - f(x_k) &\leq -\gamma \left(1 - \frac{L}{2} \gamma C \right) \sum_{k=0}^K \sum_{i=1}^n b_{k,i} g_{k,i}^2 \\ &\iff \gamma \left(1 - \frac{L}{2} \gamma C \right) \sum_{k=0}^K \sum_{i=1}^n b_{k,i} g_{k,i}^2 \leq f(x_0) - f(x_{K+1}). \end{aligned} \quad (13)$$

Since f is lower bounded, the right-hand side of (13) is uniformly bounded, so

$$\gamma \left(1 - \frac{L}{2} \gamma C\right) \sum_{k=0}^{+\infty} \sum_{i=1}^n b_{k,i} g_{k,i}^2 < +\infty \iff \sum_{k=0}^{+\infty} \langle B_k \nabla f(x_k), \nabla f(x_k) \rangle < +\infty. \quad (14)$$

Finally, by assumption B_k is positive definite, therefore (14) implies that $\sum_{k=0}^{+\infty} \|\nabla f(x_k)\|^2 < +\infty$, and thus in particular $\lim_{k \rightarrow +\infty} \|\nabla f(x_k)\| = 0$. □

D Details on the Learned Algorithm

D.1 Details on the Model

The network is exactly that described in Figure 2, we simply detail the FF and linear blocks. The first coordinate-wise FF block is made of 3 layers with output shapes (6, 12, 3), the second one has 2 layers with output shapes {12, 1}. We use ReLU activation functions after each layer except after the layer of each block. The linear layer is of size 6×1 , again with no bias. The total number of parameter of the network is 216. In comparison, the training set is made of 20 problems in dimension $n = 100$, thus $p = 216$ is much smaller than $20 \times 100 = 2000$. We also apply the algorithm to problems in dimension 500 where even for a single problem $p < 500$.

D.2 Pseudo-code

Given the model \mathcal{M} defined above, our algorithm is an enhancement of the BFGS algorithm and can be written as follows.

Algorithm 2: Learning enhanced Quasi-Newton Algorithm

given: Model \mathcal{M} defined in Figure 2 and Section D.1

input: function to minimize f , initialization x_0 , initial state

$$S_0 = \{x_{-1}, \nabla f(x_{-1}), B_{-1}\}, \text{ (with } B_{-1} = 0.8\gamma_{\text{BB}}^{(0)} \mathbb{I}_n \text{)}$$

input: number of iterations K , step-size γ (default value $\gamma = 1$).

for $k = 0$ **to** $K - 1$:

Compute $\mathcal{C}(f, x_k, S_k)$:

$$\begin{aligned} & \Delta g_k = \nabla f(x_k) - \nabla f(x_{k-1}) \\ & d_k = x_k - x_{k-1} \\ & I_k \leftarrow (B_{k-1} \Delta g_k, d_k, -\gamma B_{k-1} \nabla f(x_k)) \\ & \text{return } I_k \end{aligned}$$

Compute $\mathcal{M}(I_k, \theta)$:

return y_k

Compute *Update step* \mathcal{U} :

$$\begin{aligned} & r_k = d_k - B_{k-1} \Delta g_k \\ & B_k = B_{k-1} + \frac{1}{\langle \Delta g_k, y_k \rangle} \left[r_k y_k^T + y_k r_k^T - \frac{\langle \Delta g_k, r_k \rangle}{\langle \Delta g_k, y_k \rangle} y_k y_k^T \right] \\ & x_{k+1} \leftarrow x_k - \gamma B_k \nabla f(x_k) \end{aligned}$$

Compute *Storage* \mathcal{S} :

$$\text{ } | \quad S_{k+1} = \{x_k, \nabla f(x_k), B_k\}$$

return x_K

We mention again, that if one removes the model \mathcal{M} and replace it by $y_k = d_k$, then Algorithm 2 coincides exactly with BFGS.

E Additional Details on the Experiments

In this section we provide additional details on how to reproduce the experiments of Section 5.

E.1 Problems and Datasets

Quadratic functions. To generate a quadratic function in dimension n , we proceed as follows. We create a matrix A by first sampling its largest and smallest eigenvalues λ_{\min} , λ_{\max} uniformly at random in $[0.1, 1]$ and $[1, 50]$ respectively. We then generate the $n - 2$ other eigenvalues of A uniformly at random in $[\lambda_{\min}, \lambda_{\max}]$. This gives us a diagonal matrix D containing the eigenvalues of A . We then generate another matrix B with Gaussian $\mathcal{N}(0, 1)$ entries and make it symmetric via $B \leftarrow B + B^T$. We then compute the orthogonal matrix P that diagonalizes B and use P to build $A = PDP^T$. We then sample a vector $b \in \mathbb{R}^n$ whose entry are sampled uniformly at random in $[0, 15]$. Our function f finally reads: $f: x \in \mathbb{R}^n \mapsto \frac{1}{2} \|Ax - b\|^2$. The OOD problems are generated with the same process but different parameters for the uniform distributions.

With this process, the largest eigenvalue of $\nabla^2 f$ is $\frac{\lambda_{\max}^2}{2}$. In our experiments the largest eigenvalue in any problem is approximately 1159 and the largest condition number (the ratio between the largest and smallest eigenvalues) is approximately 15156, hence our dataset includes ill-conditioned problems.

Regularized Logistic Regression. We consider a binary logistic regression problem, as presented in [27]. For each problem, we generate two clouds of M points sampled from Gaussian distributions $\mathcal{N}(\mu_1, 1)$ and $\mathcal{N}(\mu_2, 1)$ where μ_1, μ_2 are themselves sampled from $\mathcal{N}(-1, 1)$ and $\mathcal{N}(1, 1)$ respectively. We store the coordinates of the $2M$ points in a matrix $A \in \mathbb{R}^{2M \times (n+1)}$ (a row of ones is concatenated with A , see [27]). We also create a vector $b \in \mathbb{R}^{2M}$ where each b_i takes either the value 0 or 1 depending on which class the i -th data point belong to. Given these A and b , for all $x \in \mathbb{R}^{n+1}$, the function f is defined as:

$$f(x) = \frac{1}{2M} \sum_{i=1}^{2M} \log \left(1 + e^{x^T A_i} \right) - b_i x^T A_i + \frac{\eta}{2} \|x\|^2.$$

The last term is a regularization that makes the problem strongly convex. We use a very small $\eta = 10^{-3}$. Our experiments are done for $M = 100$ and $n = 50$.

E.2 The BFGS Baseline

For a fair comparison, the BFGS algorithm is implemented exactly like Algorithm 2 but with $y_k = d_k$ instead of using learned model. We use the same strategy for initializing B_{-1} . For both algorithms we generate a random starting point $x_{-1} \in \mathbb{R}^n$, and perform a gradient descent step along $\nabla f(x_{-1})$ to obtain the true initialization $x_0 \in \mathbb{R}^n$. Both algorithms thus always start at the same x_0 with the same state $S_0 = \{x_{-1}, \nabla f(x_{-1}), B_{-1}\}$. When using our algorithm with fixed step-size (during training and in most experiments), we compare it to BFGS with fixed step-size. When using line-search, we use it for both.

E.3 Training Strategy

Training set. Our training dataset is made of 10 quadratic functions in dimension $n = 100$ created following the strategy described in Section E.1. We generate two different initializations at random for each function, yielding a training dataset of 20 problems.

Initialization of the network. We initialize the parameter θ (the weights of our layers) by following the new initialization strategy introduced in Section 5. Recall that with this strategy, before training θ our model coincides with BFGS, stabilizing the training process.

Training by unrolling. We run the algorithm for $K = 40$ iterations and use the loss function $\mathcal{L}(\theta)$ described in (5). However, we observe in practice that unrolling the last iterate (*i.e.*, computing the gradient of \mathcal{L} with respect to the last iterate K) is numerically unstable (known as the vanishing/exploding gradient problem). We mitigate this issue by computing $\mathcal{L}(\theta)$ every 5 iterations (*i.e.*, at iterations $\{5, 10, \dots, 40\}$) and by “detaching” the matrix B_k every 5 iterations (*i.e.*, neglecting

the effect that old predictions of the model have on B_k). We then average the 8 values of the loss computed along the trajectory and “back-propagate” to compute the gradient of this loss function.⁶

Training parameters. We train the model with the ADAM [37] optimizer with gradient clipping. We do not compute the full gradient $\nabla\mathcal{L}(\theta)$ but a mini-batch approximation of it by selecting only two problems at random at every iteration. We use the learning rate 10^{-4} for the FF layers and 10^{-3} for the linear layer. We save the model that achieved the best training loss on average over one epoch (a full pass on the training dataset).

E.4 Computational Architecture

We ran all the experiments on a DELL Precision 5820 Tower with 16 GiB of RAM, and an Intel XEON W-2235 CPU with 12 cores at 3.8 GHz. No GPU was used for the experiments. We used Python [61] 3.8, Numpy [67] 1.22.2 and Pytorch [54] 2.0 running on Ubuntu 20.04.

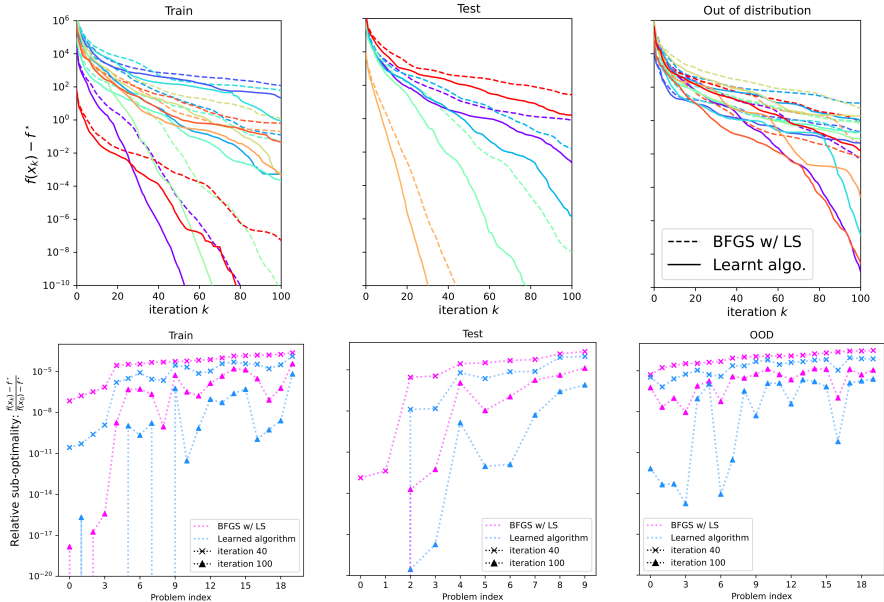


Figure 5: Same experiment as Figure 3 but we evaluate the performance of the algorithm used with line-search, *without retraining* it. Top row: sub-optimality gap against iterations on the training, test and OOD sets, each color represents a different problem. Bottom: relative sub-optimality gap for each problem after 40 and 100 iterations.

F Additional Experiments

Compatibility with line-search. Like Newton’s method, one usually wants to use QN methods with a step-size γ as close as possible to 1. This may however cause numerical instabilities (*e.g.*, in the logistic regression problem). Therefore, QN algorithms, including BFGS are often used with line-search strategy (adapting the step-size based on some rules). It is thus important to evidence that Algorithm 2 performs well when used with line-search strategies, *despite having been trained with fixed step-sizes*. The results in Figure 5 show that Algorithm 2 significantly outperforms BFGS with line-search on almost all problems, even in OOD problems. It thus appears to be highly compatible with line-search.

Visualization of the logistic regression problem. In Figure 7, we provide a 2D visualization of the type of logistic regression problems considered in Figure 4 and described in Section E. The figure shows how Algorithm 2 progressively finds a solution that separates most of the points of the two classes (perfect separation is not possible as evidenced by the figure).

⁶Since we neglect the influence that old iterates have on B_k , we do not compute true gradients of \mathcal{L} . Yet, this is acceptable since training is only a mean to obtain a good parameter θ .

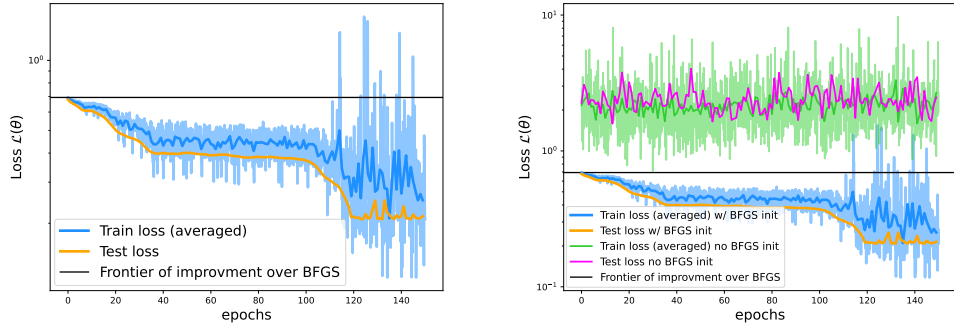


Figure 6: Left: evolution of the training loss and test loss during the training of the model of our algorithm. The blue area shows the value of the stochastic loss and the blue curve represents the average over one epoch. The test loss is computed after each epoch. The black line corresponds to $\log(2)$, any value of $\mathcal{L}(\theta)$ below this line corresponds to an improvement compared to vanilla BFGS. Right: Same figure as the left-hand side but comparison with the case where we did not initialize the model to coincide with BFGS, causing instability in training.

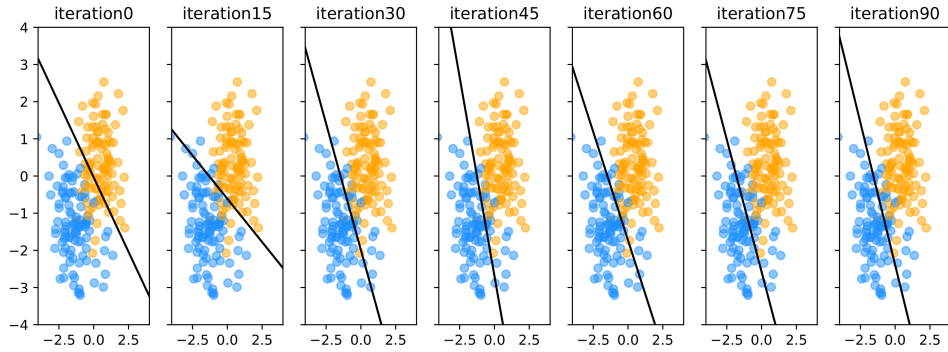


Figure 7: Evolution of the decision boundary (the black line) found by our algorithm over the iterations of the regularized logistic regression problem (see Section E). The orange and blue dots represent data points from two classes. The problem is in dimension $n = 50$, the plots only represent the first-two coordinates

Benefits of our initialization strategy. As mentioned in Section 5, we can easily find a closed-form initialization of the model $\mathcal{M}(\cdot, \theta)$ such that Algorithm 2 coincides with BFGS before training. This dramatically stabilizes the training process as shown on Figure 6 where without this initialization strategy, the average train loss stays high (despite having tuned the learning rate). This can be explained by the fact that for a random initialization, the value $f(x_K)$ produced by the algorithm will usually be very large, making it necessary to train with small learning rates, whereas with our strategy we start in a more stable region as evidenced by the smaller oscillations in early training, allowing larger learning rates.